Research article

Exploring the therapeutic efficacy of *Chlorella pyrenoidosa* peptides in ameliorating Alzheimer's disease

Shu-Mei Wang [a], Jiunn-Jye Chuu [b], Ching-Kuo Lee [a,**], Chia-Yu Chang [c,d,*]

[a] *Ph.D. Program in Drug Discovery and Development Industry, College of Pharmacy, Taipei Medical University, Taipei, Taiwan*
[b] *Department of Biotechnology and Food Technology, College of Engineering, Southern Taiwan University of Science and Technology, Tainan, Taiwan*
[c] *Department of Neurology, Chi-Mei Medical Center, Tainan, Taiwan*
[d] *Center for General Education, Southern Taiwan University of Science and Technology, Tainan, Taiwan*

ARTICLE INFO

ABSTRACT

Alzheimer's disease (AD) is one of the neurodegenerative disorders, the hallmarks of which include deposits of extracellular beta-amyloid (Aβ) as well as intracellular tau neurofibrillary tangles (NFTs) tangles. With disease progression, neuronal apoptosis combined with cerebral atrophy occurs, leading to cognitive impairment and long-term memory loss. Recently, *Chlorella* species have been identified as a functional food and are being explored for the prevention of various diseases widely studied to prevent or treat many neurodegenerative diseases. Hence, we for the first time investigated the neuroprotective effects of *Chlorella pyrenoidosa* short-chain peptides (CPPs) i.e. <1 kDa, 1–3 kDa, 3–10 kDa, and >10 kDa on the *in vitro* and *in vivo* neuronal injury models. Our *in vitro* results showed that CPP with a molecular weight of 1–3 kDa and 3–10 kDa could elevate the survival rate of $A\beta_{1\text{-}42}$ or L-Glutamic acid-injured N2A cells. These treatments also inhibited Aβ and tau NFTs in N2A cells and prevented progressive neuronal cellular damage by suppressing inflammatory cytokines such as PGE2, iNOS, IL-6, TNF-α, COX-2, IL-1β, TGF-β1, and NF-κB. Further, our *in vivo* $A\beta_{1\text{-}42}$-induced AD mice model demonstrated that 1–3 kDa or 3–10 kDa CPP could improve spatial cognition and learning memory. We also observed a decreased cell loss ratio in CA1-CA3 hippocampal regions. Taken together, our findings imply that CPPs may exert their anti-AD impact through anti-inflammatory, and anti-amyloid activities via reducing APP and tau NFT.

1. Introduction

Alzheimer's disease (AD) is one of the most prominent and slowly progressive neurodegenerative disorders leading to dementia and loss of cognitive function [1,2]. The increasing prevalence of AD is a major cause of memory loss, poor health, and deteriorating quality of life (QoL) among the aging population [3,4], and approximately 50 million people are suffering from AD or related dementia throughout the globe [3,5]. It has been projected that in the United States of America (USA) alone the cases of AD will increase from 6.2 million to 13.8 million by 2060 [6].

The major pathological cause of AD is the accumulation and aggregation of β-amyloid (Aβ) protein specifically β_{1-42} and tau protein within brain cells [3,7]. Though the exact mechanism of AD progression remains to be explored, various aspects of the disease progression have been highlighted. Pathological changes such as oxidative damage, active inflammatory cells, neurofibrillary tangles of microtubules associated with tau protein, amyloid plaques, and synaptic and neuronal loss are some characteristic features of AD [7]. The presence of amyloid plaque and microfibrillar tangle are two critical factors that contribute to brain atrophy [2]. It has been established that Aβ plays the most critical role in the initiation and progression of AD [8]. The amyloid precursor protein (APP) is a transmembrane in the brain that is cleaved into various Aβ fragments by α-, β-, and γ-secretases [8,9]. The β-secretase cleavage generates a C-terminal APP fragment of 99 amino acids (C99) which finally leads to the generation of final Aβ-40 and the Aβ-42 fragments with 40 and 42 amino acids, respectively [9–11]. The misfolding of Aβ results in aggregation in cerebrovasculature, neocortex, and the hippocampus region resulting in extracellular Aβ accumulation in senile plaque [9,12,13]. Furthermore, Aβ aggregates increase the level of reactive oxygen species (ROS), which oxidizes several lipids and proteins resulting in a loss in membrane integrity and neuronal functional proteins such as creatine kinase and glutamine synthetase [2,14,15]. Notably, oxidized lipid reaches to different neuron regions severely impacting their function by loss of Ca^{2+} homeostasis, inhibition of glial cell Na^+-dependent glutamate and ion-motive ATPases, and disruption in signaling pathways [16–18]. An elevated level of Aβ aggregation induces an inflammatory response, release of inflammatory molecules such as complement factors, chemokines, eicosanoids, and chemokine, and immune response via microglia activation leading to the destruction of functional neurons [2,19–22].

Currently, there are mainly two types of drug-based treatments for AD which functions either by inhibiting cholinesterase or antagonizing the effects of N-methyl D-aspartate (NMDA).

[1]. However, the efficacy of these drugs remains inadequate and is associated with various adverse events such as gastrointestinal disorders, hepatoxicity, dizziness, nausea, and vomiting [23,24]. Besides, the β-secretase (BACE-1) inhibitors are effective in suppressing Aβ aggregation, however, these drugs are not explored due to their toxic nature. Thus, considering the limitation of drug treatment, alternative efficacious therapies providing long-term treatment are being explored.

Recently, microalgal research has shown their richness in bioactive molecules such as carotenoids, fatty acids, sterols, polysaccharides, and phenolic compounds in exhibiting therapeutic effects on cancer, viral infection, and hypocholesterolemia and other disorders [23,25–29]. *Chlorella* species is one of the algal species with therapeutic and nutritional values owing to the presence of an antioxidant, anticholinesterase, and anti-amyloidogenic molecules in them [23,30,31]. Specifically, *Chlorella pyrenoidosa* (*C. pyrenoidosa*) is a rich source of hypotensive and hypoglycemic peptides [32]. The hydrolyzed peptides of *C. pyrenoidosa* (CPPs) have also been demonstrated with therapeutic properties such as antioxidant, anti-inflammatory, antihypertensive, immunostimulant anticarcinogenic, anti-atherosclerotic, antihypertensive, and immunomodulatory potential activities [32,33]. Additionally, *C. pyrenoidosa* has demonstrated its potential role in lowering high blood pressure, glucose, and serum cholesterol along with ameliorating immune response [32,34–36].

Considering the therapeutic significance of *chlorella sp.* in various diseases, we derived different molecular weights of CPP and evaluated their effectiveness in the treatment of AD by investigating the inhibitory activities against Alzheimer's-like pathologic changes through various *in vitro* and *in vivo* studies.

2. Materials and methods

2.1. Chlorella pyrenoidosa peptides (CPPs)

Chlorella Pyrenoidosa dry powder was purchased from Gong-Bih Enterprise Co. Ltd. (Taiwan). 100 g dry powder of *Chlorella Pyrenoidosa* covered with d.d.H₂O 1:10 (v/v) and placed in a sterilizer for hot water extraction (120 °C, 50 min), cooled for 24 h, filtered through a 90 mm pore size filter membrane. The supernatant was mixed with 75% ethanol in a 1:1 vol ratio, standing at 4 °C for 24 h. Next, the supernatant was taken, and 50 ml of pepsin (1 mg/ml pepsin) was added and centrifuged (1.2 rpm, 10 min). The supernatant was taken and lyophilized (−40 °C, 24 h). The obtained chlorella extract powder was re-dissolved with 50 ml of d.d.H₂O, mixed with ethyl acetate in a 1:1 vol ratio, and placed in a separatory funnel for stratification. The solution was collected and lyophilized in a freeze dryer (−40 °C, 24 h). Finally, the chlorella extract powder was re-dissolved into 50 ml of d.d.H₂O, separated, and purified by 1, 3, and 10 kDa molecular weights of hollow fiber filter modules, respectively. The CPP formula was provided by Tai-Jian Biotech Co. Ltd. (Taiwan).

2.2. Analysis and identification of CPPs

Purified CPPs with molecular weights <1 kDa, 1–3 kDa, 3–10 kDa, and >10 kDa were analyzed by Q-TOF mass spectrometer for amino acid composition analysis and peptide sequence identification.

2.3. In vitro cell culture

The mouse neuroblastoma cell line N2A (ATCC® CCL 131™) was provided by Professor Ming-Chang Chiang, Department of Life Science, Fu-Jen University (Taiwan). The cells were maintained in 90% MEM medium, containing 0.1 mmol/L nonessential amino acids and 1 mmol/L sodium pyruvate supplemented with 10% heat-inactivated fetal bovine serum, 2 mmol/L L-glutamine, 1.5 g/L sodium bicarbonate in 75 T culture flasks. For experiments, the cells were subcultured in microtiter plates in the above culture medium in an incubator (95% air and 5% CO2 at 37 °C, 90% humidity), and the medium was changed every 2 days until analysis.

The mouse brain microglial cell line BV2 (ICLC ATL03001) was provided by Professor Ming-Chang Chiang, Department of Life Science, Fu-Jen University (Taiwan). The cells were maintained in 90% DMEM medium, containing 10 mM HEPES, 1 mmol/L sodium pyruvate supplemented with 10% heat-inactivated fetal bovine serum, 1% penicillin-streptomycin, 2 mmol/L L-glutamine and pyridoxine hydrochloride. For experiments, the cells were subcultured in microtiter plates in the above culture medium in an incubator (95% air and 5% CO_2 at 37 °C, 90% humidity), and the medium was changed every 2 days until analysis.

The mouse macrophage cell line RAW264.7 (ATCC® TIB 71™) was purchased from the Food Industry Research and Development Institute (Taiwan). The cells were maintained in a 90% DMEM medium, containing 10% heat-inactivated fetal bovine serum, 1.5 g/L sodium bicarbonate, 4 mmol/L L-glutamine, and 4.5 g/L glucose. For experiments, the cells were subcultured in microtiter plates in the above culture medium in an incubator (95% air and 5% CO_2 at 37 °C, 90% humidity), and the medium was changed every 2 days until analysis.

2.4. Atorvastatin formulation

The medicine atorvastatin was purchased from Echo Chemical Co. Ltd. (Taiwan). Atorvastatin was dissolved in d.d.H_2O to prepare a stock concentration of 10 mM, sealed with paraffin, and placed at 4 °C in dark for further experiments.

2.5. Cell viability assessment

The viability of N2A cells was measured by the reduction of MTT [3-(4,5-dimethylthiazol-2-yle)2,5-mdiphenyltetralozium bromide]. Cells were harvested when in the exponential growth phase, cultured in 100 μL of fresh medium at 1×10^5 cells/well in 96-well plates. Cells were incubated in 5% CO2 at 37 °C for 24 h. After that, the N2A cells were induced with 10 μM concentration of β-amyloid1-42 (Aβ$_{1-42}$) (Cayman Chemical Company 1.800.364.9897) and treated with d.d.H2O, Atorvastatin (10 μM), <1 kDa, 1–3 kDa, 3–10 kDa and >10 kDa *Chlorella Pyrenoidosa* peptides (10 μg/mL) for 24 h, respectively. Moreover, BV2 and RAW264.7 cells were induced with 20 μl (2 μg/ml) lipopolysaccharide (LPS) (Sigma-Aldrich® 297-473-0) for 3 h, and treated with d.d.H2O, Atorvastatin (10 μM), <1 kDa, 1–3 kDa, 3–10 kDa and >10 kDa *Chlorella Pyrenoidosa* peptides (10 μg/mL) for 24 h. BV2 conditioned medium or BV2 (100 μl) + RAW264.7 (100 μl) conditioned medium were respectively replaced into the N2A cell's reaction medium that had pretreated with 10 μM concentration of Aβ$_{1-42}$ (24 h). The reaction was continued for 24 h to estimate the cell viability. Cell proliferation was then assayed using the MTT assay as follows. PBS solution (20 μL) containing 5 mg/mL MTT was added to each well; cells were further incubated for 4 h and then solubilized in 100 μL DMSO for optical density measurements at 570 nm. Cell survival was expressed as the ratio of the number of MTT-treated cells to the number of control cells (% of control).

2.6. Cellular cytokines level analysis by ELISA

N2A cells were induced with 10 μM of Aβ$_{1-42}$ and 2 mM of L-Glutamic acid (Echo Chemical Co. Ltd) for 24 h, respectively. BV2 and RAW264.7 cells were induced with 20 μl (2 μg/ml) LPS for 3 h, and treated with d.d.H_2O, atorvastatin (10 μM), <1 kDa, 1–3 kDa, 3–10 kDa and >10 kDa *Chlorella Pyrenoidosa* peptides (10 μg/mL) for 24 h. The cellular cytokines levels in the cell culture medium were measured using mouse PGE2, IL-6, iNOS, TNF-α, COX-2, IL-1β ELISA Kit (Enzo Biochem, USA), according to the enzyme-linked immunosorbent assay manufacturer's protocol.

2.7. Cellular cytokines mRNA expression analysis by RT-PCR

BV2 and RAW264.7 cells were induced with 20 μl (2 μg/ml) LPS for 3 h, and treated with d.d.H_2O, atorvastatin (10 μM), 1–3 kDa, and 3–10 kDa CPP (10 μg/mL, 100 μg/mL) for 24 h. The cellular cytokines mRNA expression was measured by using RT-PCR specific primers for IL-6, TGF-β1, TNF-α, and NF-κB (Enzo Biochem, USA), according to the reverse transcription-polymerase chain reaction manufacturer's protocol.

2.8. Cellular protein level analysis by western blot

N2A cells were induced with 10 μM of Aβ$_{1-42}$ and 2 mM of L-Glutamic acid for 24 h, respectively. Moreover, BV2 and RAW264.7 cells were induced with 2 μg/ml LPS for 3 h and treated with d.d.H_2O, atorvastatin (10 μM), 1–3 kDa, 3–10 kDa *Chlorella Pyrenoidosa* peptides (10 μg/mL) for 24 h. BV2 conditioned medium or BV2 + RAW264.7 conditioned medium were respectively replaced into the N2A cell's reaction medium that had pretreated with 10 μM of Aβ$_{1-42}$ or 2 mM of L-Glutamic acid (24 h). The reaction was continued for 24 h to estimate the cellular protein levels. Tau proteins and amyloid precursor proteins (APP) were measured using BCA Protein Assay Kit (Enzo Biochem, USA), according to the Western blot manufacturer's protocol.

2.9. Animal preparation

Male ICR mice at 5 weeks of age were purchased from BioLASCO Taiwan Co., Ltd. All animals were maintained in laminar flow cabinets with free access to food and water under specific pathogen-free conditions in facilities approved by the Accreditation of Laboratory Animal Care and following the Institutional Animal Care and Use Committee (IACUC) of the Animal Research Committee (STUST-107-2) of the Southern Taiwan University of Science and Technology, Tainan, Taiwan. Six mice per cage were fed with mouse

chow and water ad libitum. The mice acclimatized to the 12:12 h light-dark cycle conditions in the cages. Animals were kept in a housing facility for a 2-week acclimation period before $A\beta_{1-42}$ is infused into mice brains to mimic Alzheimer's disease.

The mice were fed with Saline, atorvastatin, 1–3 kDa, and 3–10 kDa CPPs for 14 days. Then, all subject mice were anesthetized by intraperitoneal injection of sodium pentobarbital (50 mg/kg), and then placed on the animal stereotaxic apparatus to locate the left lateral ventricle. Taking bregma on the cranial bones as the center, the lateral ventricle was localized and drilled at the position of 0.4 mm vertical axis and 1.0 mm horizontal axis. $A\beta_{1-42}$ Oligomer (400 pmol) in 35% Acetonitrile/0.1% Trifluoroacetic Acid (pH 2.0) solution was injected with 5 μl Hamilton Microsyringe I.C.V. into the Bilateral ventricle regions to a depth of 2.0 mm from the cranial bones. The gasket was fixed on the cranial bones with bioadhesive and finally sutured with a sewing needle. The mice were kept in a 37 °C room for several hours to prevent hypothermia, and then returned to the rearing cage for care. Further animal behavioral experiments were started after they returned to their normal activities (about 5 days). After completion, all subject mice were sacrificed for histochemical staining (H&E) examination.

2.10. Animals, treatment, and experimental design

All mice were randomized into 5 groups (n = 6): (1) Sham: without $A\beta_{1-42}$ treatment; (2) Saline + $A\beta_{1-42}$: animals given intragastrically with a single dose of Saline followed by intracerebroventricular injection of $A\beta_{1-42}$ (5 μM); (3) atorvastatin + $A\beta_{1-42}$: animals given intragastrically with a single dose of atorvastatin (5 mg/kg) followed by intracerebroventricular injection of $A\beta_{1-42}$ (5 μM) (4) CPP 1–3 kDa + $A\beta_{1-42}$: animals intragastrically with a single dose of 1–3 kDa CPPs (100 mg/kg) followed by intracerebroventricular injection of $A\beta_{1-42}$ (5 μM). (5) CPP 3–10 kDa + $A\beta_{1-42}$: animals intragastrically with a single dose of 3–10 kDa CPPs (100 mg/kg) followed by intracerebroventricular injection of $A\beta_{1-42}$ (5 μM).

2.11. Spatial tracking in the water maze

The Reference Memory Task is one of the evaluation methods of the Hidden-Platform Acquisition Train, which is mainly used to measure the learning and memory ability of animals in the water maze (an evaluation method of long-term memory ability), the experiment lasted for 4 days. The diameter of the circular swimming pool is 140 cm, and the height is 45 cm. The swimming pool has a diameter of 12 cm and a height of 25 cm movable rest platform. Before the experiment, the swimming pool must be filled with water to 27 cm level height. The pool area is divided into four quadrants (I, II, III, and IV), and 5 starting points are set. The resting platform is placed at the center point of any quadrant. A half hour before the experiment, the mice were placed in the room where the water maze was located to adapt to the environment. Each mouse was trained twice a day, the resting platform was fixed on one of the quadrants, and the animals headed outwards and randomly entered the four entry points. During the experiment, a camera was set up above the central point of the swimming pool to record the swimming path and latency of the experimental mice in each quadrant. Further statistical analysis (Animal Video Behavior System) was performed on the time/path length, average movement speed, times of passing through the virtual platform, and latency time on the virtual platform of the experimental mice in a specific area. The maximum duration of each test is 180 s.

2.12. Passive avoidance test

The composition of the passive avoidance test equipment is an aluminum shuttle cage of 72 (length) × 34 (width) × 24 (height) cm3 (Coulbourn Instruments Model E10-15) and is divided into a bright room and a dark room, with a guillotine door (Coulbourn Instruments Model E10-15GD) of 7.5 (L) × 6.5 (W) cm^2 in the center, and bottom of the shuttle cage is setting with metal rods arranged in parallel with an interval of 1 cm, to connect the current device. First, the mice were placed in a bright room, and after 10 s of adaptation, the small gate of the septum was opened to allow them to explore freely. Once the mice entered the dark room, the small gate was quickly closed and conducted low-voltage 33 V with a 5-s electric shock to the mice's feet. It lasts 5 s for one electric shock, three times in total, and the learning training was completed. After 24 h, the animal was placed in the bright room, and the gate was opened at the same time, step-through latency of the animal in the bright room was recorded. The longer the latency time in the bright room, the better the learning training and memory ability. In this experiment, the infrared rapid scanning detection system in the Shuttle Avoidance Instrument was used to accurately and timely measure the shuttle times and latency of mice. The maximum duration of each test is 180 s.

2.13. Hematoxylin and eosin (H&E) staining

The hippocampal tissue of mice injected with $A\beta_{1-42}$ in the brain was taken out and soaked in formalin for two days. After dehydrating and waxing, the tissue was embedded and sliced to 5 mm thickness, well spread, and attached to the glass slide through 40 °C warm water. Before staining, tissue slices were placed in a 60 °C oven for dewaxing for 1 h, then washed with xylene and dehydrated with alcohol gradient, followed by the H&E dyeing step manufacturer's protocol. The changes in cell morphology in the CA1-CA3 region of mice's hippocampus were observed by microscope.

2.14. Statistical analysis

SigmaPlot 14.0 software was used for experimental data processing and drawing. The statistical representation of experimental

results was mean ± standard error (mean ± SE). For the i*n vitro* experiments, the significant difference between groups was calculated using a *t*-test in SigmaPlot software. Whereas for *In vivo* experiments, One-way ANOVA plus post-hoc test (Scheffe method) was employed to calculate the P value. The P values less than 0.05 were considered statistically significant. Image J was employed for quantifying Western Blot and RT-PCR data, while SigmaPlot 14.0 was used for statistical analysis.

3. Results

3.1. Effect of CPPs on the cell survival of N2A, BV2, and RAW264.7 cell lines

To determine the cytotoxic impact of CPPs, the N2A, BV2, and RAW264.7 cell lines were treated with CPPs <1 kDa, 1–3 kDa, 3–10 kDa, and >10 kDa, and thereafter MTT assays was done. The used concentrations of CPPs in each group were 100 and 1000 μg/ml. The results revealed higher toxicity of CPPs at a concentration of 1000 μg/ml than 100 μg/ml (Fig. 1A, B, and C). All the CPP groups showed significantly reduced cell survival (P < 0.05) at a concentration of 1000 μg/ml, with the highest efficacy of >10 kDa in lowering the survival rate of RAW264.7 at both concentrations of 100 and 1000 μg/ml. Therefore, 100 μg/ml was selected as the optimum dose of CPP in further experiments.

3.2. Impact of CPPs on $A\beta_{1-42}$ and LPS-induced cytotoxicity

We further assessed the effect of CPP on β-amyloid 1–42 ($A\beta_{1-42}$). The abnormal cleavage of amyloid precursor protein (APP) results in the peptide fragment of $A\beta_{1-42}$ which when deposited in a specific brain area may induce memory loss and cognitive impairment thereby mimicking the AD pathophysiology [37–39]. First, the MTT assay was performed to assess the impact of CPPs on $A\beta_{1-42}$-induced toxicity in N2A cells. It was observed that compared to atorvastatin, all CPP groups 1–3 kDa and 3–10 kDa were more effective in improving cell viability (Fig. 2A). Additionally, 3–10 kDa CPP was the most effective candidate against $A\beta_{1-42}$ (10 μM)-induced cytotoxicity. Further, the conditioned medium from LPS-induced BV2 cells was used as a replacement medium for N2A cells pre-conditioned with $A\beta_{1-42}$ (10 μM). Results revealed that CPPs and atorvastatin improved cell viability (Fig. 2B). Further, the cell viability of N2A cells in LPS-induced BV2 and RAW264.7 conditioned medium was also improved. CPPs had nearly similar efficacy to atorvastatin in maintaining N2A cell viability in BV2+RAW264.7 conditioned medium (Fig. 2C).

3.3. Effect of CPPs on level of N2A and BV2-related inflammatory factors PGE2, IL-6, and iNOS

In the central nervous system, inflammation is closely associated with neurodegenerative disorders, and neuronal cell populations in brain areas are activated during neuroinflammation [40]. In this study, we used the classic preclinical AD models of $A\beta_{1-42}$-induced N2A cells and LPS-induced BV2 microglia to investigate the neuroprotective effects of CPPs. We specifically aimed to check whether BV2 cells exert any indirect toxic effects on *N2A* cells by producing inflammatory cytokines such as PGE2, IL-6, and iNOS associated. N2A cell line was induced with L-Glutamic acid (2 mM) and $A\beta_{1-42}$ (10 μM) for 24 h, respectively. LPS has been reported to induce inflammation in microglia [41]. Therefore, The BV2 cell line was induced with LPS (2 μg/ml) for 3 h before being exposed to atorvastatin (10 μM) and CPP groups (10 μg/ml). Our ELISA results demonstrated that the LPS-induced BV2 cell line expressed inflammatory cytokines such as PGE-2, IL-6, and iNOS. However, it was observed that atorvastatin and all CPP groups significantly lowered the expression of these cytokines. The expression of PGE2 was significantly lowered by the CPP (1–3 kDa) in comparison to other CPP groups and atorvastatin (10 μM) (Fig. 3A). However, the inflammatory factor IL-6 was significantly downregulated in all groups (Fig. 3B); the downregulation effect of atorvastatin (10 μM), and CPP (3–10 kDa) at 10 μg/ml were comparable and higher than other CPP groups. Notably, the expression level of iNOS significantly lowered in CPP 3–10 kDa, and the inhibitory effect was the highest
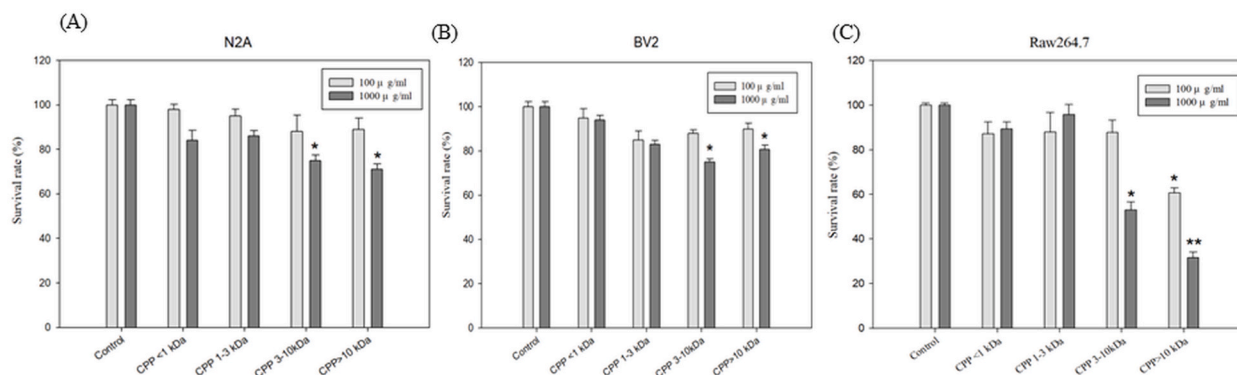

Fig. 1. Anti-cytotoxic impact of CPP on (A) N2A (B) BV2, and (C) RAW264.7 cells for 48 h. Control group was compared with CPP <1 kDa, 1–3 kDa, 3–10 kDa and >10 kDa (n = 3), and the concentrations of CPP in each group were designated to be 100 and 1000 μg/ml. CPP: Chlorella peptides, *P < 0.05 compared with control.
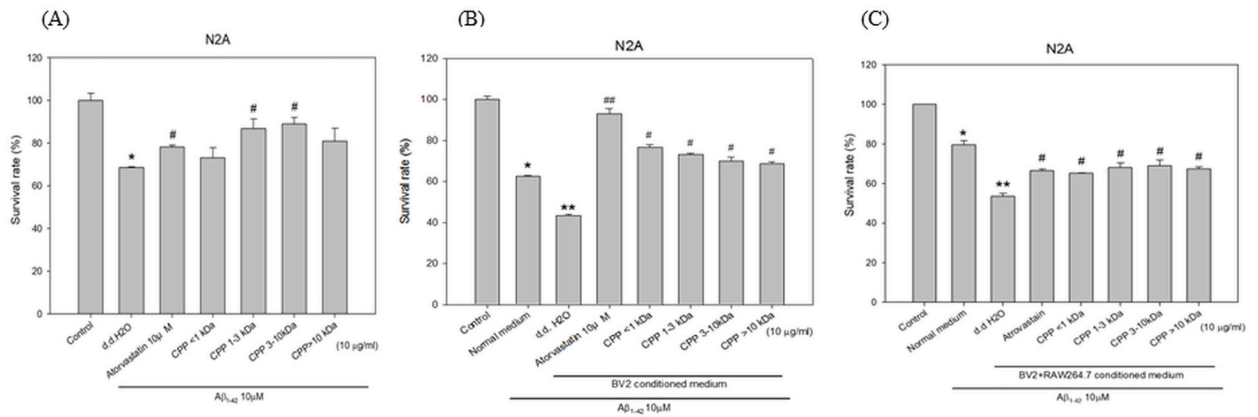
Fig. 2. Assessment of cell survival (%) of N2A in (A) Aβ$_{1-42}$ medium (B) BV2-conditioned medium, and (C) BV2 and RAW264.7 mixed conditional medium. These levels were determined after cells were treated with atorvastatin, CPP<1 kDa, CPP 1–3 kDa, CPP 3–10 kDa, and CPP>10 kDa, where d.d.H$_2$O was considered as a control. Each group of CPPs concentration was designated as 10 μg/ml (n = 3), *P < 0.05 compared to control, #P < 0.05 compared to d.d.H$_2$O).

among all groups (Fig. 3C). In addition, the expression of inflammatory factors PGE2, IL-6, and iNOS was negligible in L-Glutamic acid (2 mM) and Aβ$_{1-42}$ (10 μM) induced N2A cells for 24 h (Fig. 3A, B, and C).

3.4. Effect of CPPs on level of N2A and RAW264.7-related inflammatory factors

Determination of inflammatory factors such as TNF-α, COX-2, and IL-1β in N2A and RAW264.7 cell lines is critical to evaluate the anti-inflammatory effect of CPPs. Our ELISA assay revealed that the LPS (2 μg/ml)-treated RAW264.7 cells showed high expression of TNF-α (Fig. 4A), COX-2 (Fig. 4B), and IL-1β (Fig. 4C). Atorvastatin (10 μM) and CPP groups (10 μg/ml) downregulated the level of TNF-α in induced RAW264.7. The efficacy of CPP groups was significantly higher than atorvastatin in reducing the level of TNF-α though no significant difference was observed among the activity of CPP groups (Fig. 4A). Notably, atorvastatin and CPPs significantly lowered the expression of the inflammatory factor COX-2. The downregulation efficacy of CPP was significantly higher than atorvastatin (Fig. 4B). Further, CPPs and atorvastatin were significantly effective in lowering the level of IL-1β. Besides, the efficacy of CPP was higher than atorvastatin. This effect was remarkable in the 1–3 kDa group (Fig. 4C). In addition, no presence of TNF-α, and an increased level of IL-1β was found in the N2A cell line, induced with L-Glutamic acid (2 mM) and Aβ$_{1-42}$ (10 μM) for 24 h (Fig. 4A and C). However, a significant level of COX-2 was detected in L-Glutamic acid (2 mM) and Aβ$_{1-42}$ (10 μM)-induced N2A cells (Fig. 4B).
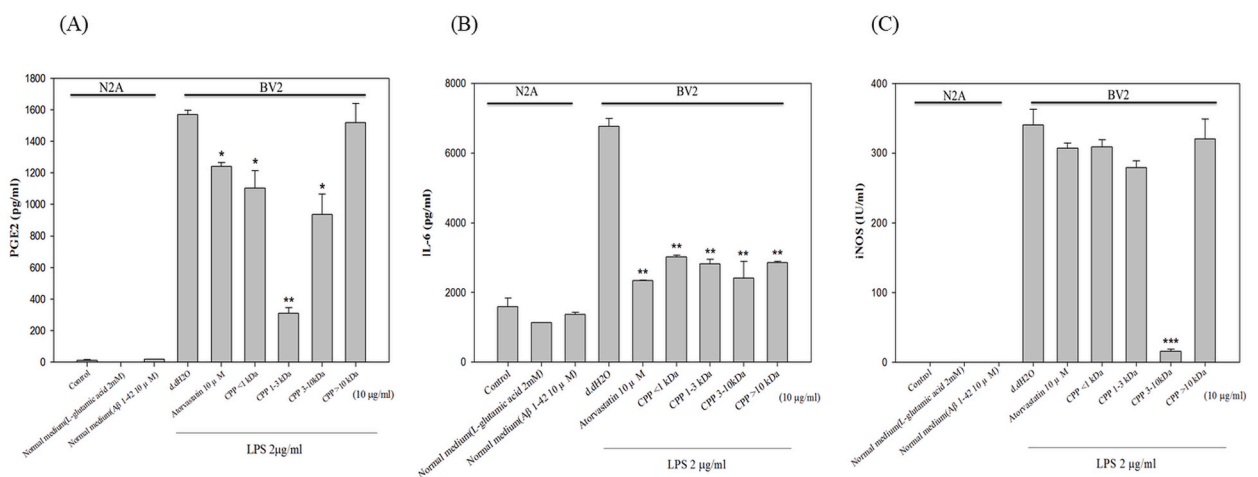

Fig. 3. Inflammatory profile determination through detection of (A) PGE2, (B) IL-6, and (C) iNOS in N2A and BV2 cells. Inflammation in N2A was induced for 24 h with L-Glutamic acid (2 mM) and Aβ$_{1-42}$ (10 μM), respectively. While inflammation in BV2 was induced with LPS (2 μg/ml) for 3 h. Inflammatory factor levels were determined after cells were treated with atorvastatin, CPP<1 kDa, CPP 1–3 kDa, CPP 3–10 kDa, and CPP>10 kDa for 24 h, where d.d.H$_2$O was considered as a control. Each group of CPP concentrations was designated to be 10 μg/ml (n = 3), *P < 0.05 **P < 0.01 compared to d.d.H$_2$O.
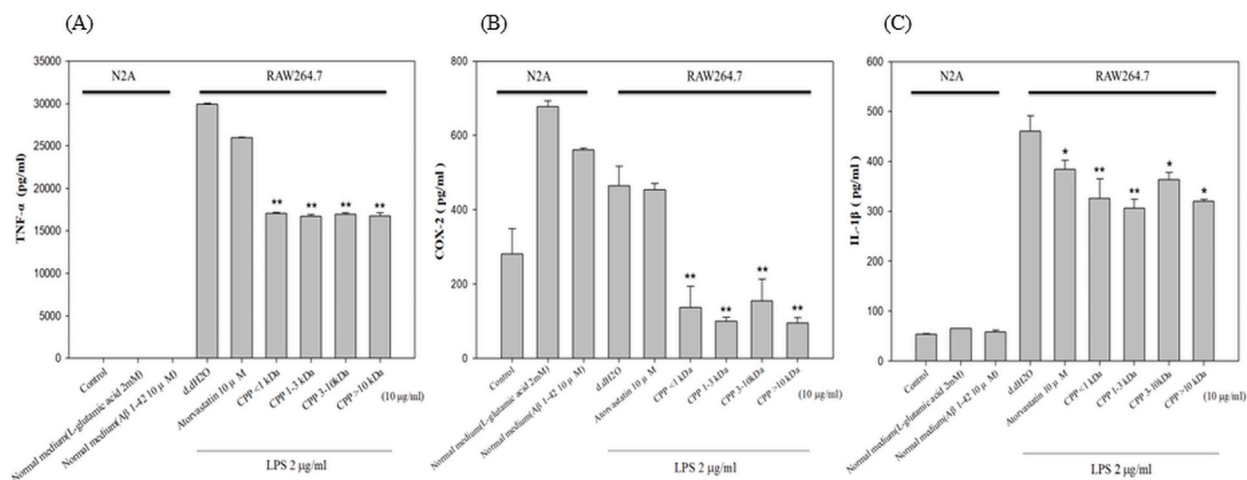
Fig. 4. Inflammatory profile determination by detecting (A) TNF-α, (B) COX-2, and (C) IL-1β in N2A and RAW264.7 cells. Inflammation in N2A was induced for 24 h with L-Glutamic acid (2 mM) and Aβ$_{1-42}$ (10 μM), respectively, and related inflammatory factors were detected in the N2A cell culture medium. The inflammation in RAW264.7 cells was induced with LPS (2 μg/ml) for 3 h, and then administered with atorvastatin and various groups of CPPs for 24 h. Inflammatory factor levels were determined after cells were treated with atorvastatin, CPP<1 kDa, CPP 1–3 kDa, CPP 3–10 kDa, and CPP>10 kDa where d.d.H$_2$O was considered as a control. Each group of CPP concentrations was designated to be 10 μg/ml (n = 3), **P < 0.01 compared to d.d.H$_2$O.

3.5. CPPs regulate the expression level of inflammatory factors

We measured the effect of CPPs on the expression level of inflammatory profiles such as IL-6, and TGF-β in BV2, and TNF-α, and NF-κB in the RAW264.7 cell line. In the induced BV2 cell line, CPP 3–10 kDa (100 μg/ml) was the most effective in downregulating the expression of IL-6 and TGF-β (Fig. 5A and B). A similar pattern was also observed in the induced RAW264.7 cell line, in which CPP 1–3 kDa and 3–10 kDa (100 μg/ml)] significantly lowered the expression of TNF-α, and NF-κB (Fig. 5C and D). Additionally, CPP 3–10 kDa (100 μg/ml) showed the most effective role in downregulating the expression of the inflammatory profile associated with microglia or macrophages caused by endotoxins.

3.6. Effect of CPPs on APP and tau protein

Aβ deposition and neurofibrillary tangles synthesized via highly phosphorylated tau protein are contemplated as major pathological hallmarks of AD [42]. The expression level of APP and tau protein was significantly lowered by the CPPs and atorvastatin in the Aβ$_{1-42}$ Injured-N2A cell line with BV2 conditioned medium. Our results indicate that CPP 1–3 kDa, and CPP 3–10 kDa at 10 μg/ml were most effective in downregulating the expression of APP (Fig. 6A) and tau protein (Fig. 6B). Similarly, the expression level of APP (Fig. 6C) and tau protein (Fig. 6D) were downregulated in Aβ$_{1-42}$ Injured-N2A cells cultured in BV2 and RAW264.7 conditioned medium. The efficacy of all CPPs was equivalent in controlling the expression of APP and tau protein in Aβ$_{1-42}$ Injured-N2A with BV2 and RAW264.7 conditioned medium. Further, the CPP groups were also effective in reducing the expression of APP (Fig. 6E) and tau protein (Fig. 6F) in L-Glu Injured-N2A with BV2 and RAW264.7 conditioned medium. All these results indicate the APP and tau protein-inhibiting potential of CPPs.

3.7. Effect of CPPs on spatial memory and learning

To assess the impacts of CPPs on spatial memory and learning, we have conducted a mouse water maze (MWM) behavior test. Mice were injected with Aβ$_{1-42}$ (5 μM) for 14 days and further administered with saline, atorvastatin, and CPPs. Atorvastatin and CPPs 1–3 kDa and 3–10 kDa were effective in improving the mouse's spatial learning and memory. Specifically, The CPPs-treated mice effectively searched their way to find the target quadrant (Fig. 7D, and E). Similarly, the atorvastatin-fed mice also efficiently reached the targeted quadrant (Fig. 7C) in comparison to the saline (Fig. 7B) and sham group (Fig. 7A). Thus, we found that CPPs 1–3 kDa and 3–10 kDa were similar to atorvastatin in improving learning and memory.

The MWM test further demonstrated that mice injected with atorvastatin and CPP groups of 1–3 kDa and 3–10 kDa showed a reduction in latency for searching hidden platform within 180 s (Fig. 8A), entrance into the dark compartment with electric shock (Fig. 8B), and intention of entering the dark compartment with electric shock (Fig. 8C) compared to sham and saline mice groups. CPP 1–3 kDa was most effective in reducing the latency of search for the hidden platform and increasing the latency of entrance into the dark compartment with electric shock. However, CPP 3–10 kDa fed mice showed a similar pattern to the atorvastatin in increasing the latency of entrance into the dark compartment. Notably, CPP 1-3 kDa-fed mice recorded a significantly lower number of intentions to enter the dark compartment compared to saline groups. A similar pattern was also observed for atorvastatin and CPP 3–10 kDa but at
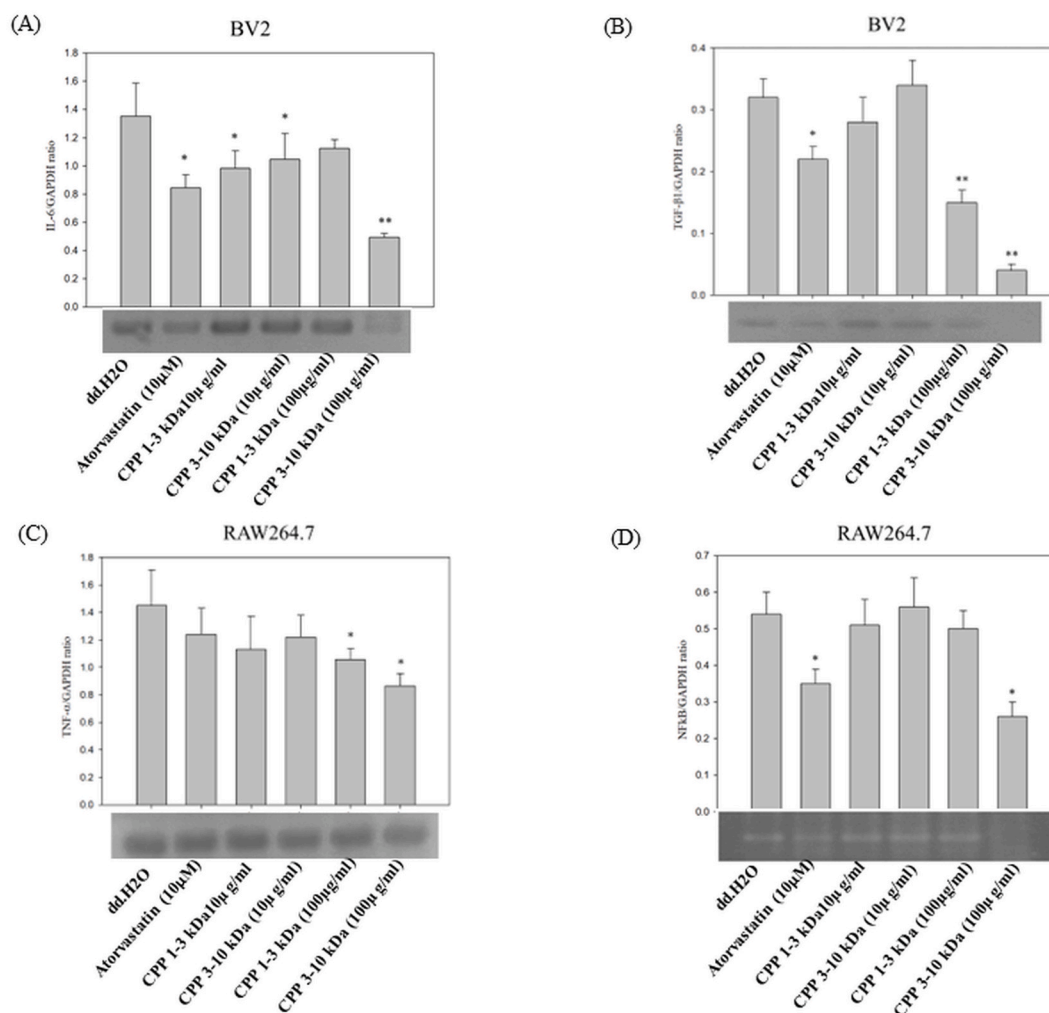
Fig. 5. Gene expression-based inflammatory profile. Levels of (A) IL-6, and (B) TGF-β1 in BV2 cells. The magnitude of (C) TNF-α and (D) NF-κB in RAW264.7 cells. These levels were determined after cells were treated with Atorvastatin, CPP 1–3 kDa (10 μg/ml), CPP 3–10 kDa (10 μg/ml), CPP 1–3 kDa (100 μg/ml), CPP 3–10 kDa (100 μg/ml) where d.d.H$_2$O was considered as a control. CPP concentrations were designated as 10 and 100 μg/ml in each group. (n = 2) *P < 0.05 **P < 0.01 compared to d.d.H$_2$O.

an equivalent level within both groups.

3.8. Histologic assessment for cell loss in the CA1-CA3 region

To evaluate the efficacy of CPPs in restoring the cell density in the CA1-CA3 region of the mouse hippocampus, histological analysis was performed. The HE staining showed the induction of mice with Aβ$_{1-42}$ (5 μM) after feeding with CPP 1–3 kDa, 3–10 kDa, and atorvastatin for 14 days. Notably, CPPs and atorvastatin were effective in improving cell density in mice hippocampus regions compared to control (saline) groups (Fig. 9A–E). Additionally, the histological assessment showed a significant reduction in lacunar infraction and cell loss (indicated by black arrows) among mice fed with CPPs and atorvastatin.

4. Discussion

As various studies have indicated a threefold increase in Alzheimer-related dementia by 2050, an effective therapeutic agent without exerting any adverse effect should be urgently developed [43]. Therefore, we attempted to investigate the anti-Alzheimer's activity of microalgae as functional foods owing to their pharmacological properties such as anti-obesity, antioxidant, anti-inflammatory, immunomodulatory, and anti-cancer [44]. These pharmaceutical characteristics of microalgae could be an effective way to provide comprehensive therapy for neurogenerative disorders such as amyotrophic lateral sclerosis (ALS), Huntington's disease (HD), Parkinson's disease (PD), and Alzheimer's disease (AD). Chlorella is a microalga and rich source of protein and
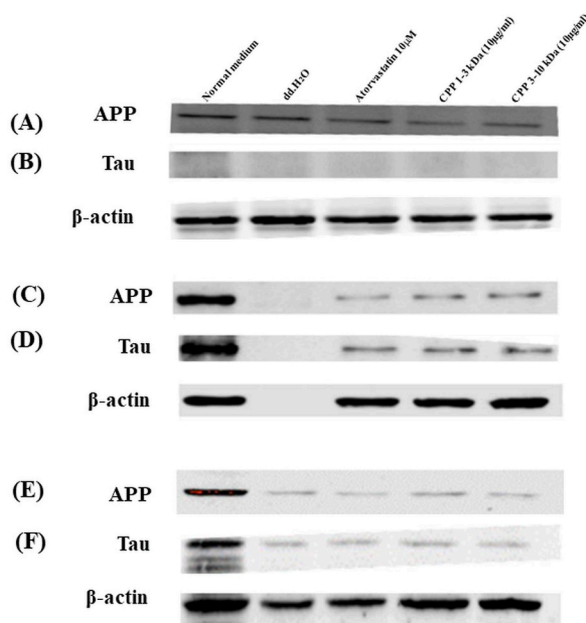
Fig. 6. CPP (on APP and Tau protein expression in (A–B) Aβ$_{1-42}$ Injured-N2A with BV2 Conditioned Medium. (C–D) Aβ$_{1-42}$ Injured-N2A with BV2 and RAW264.7 Conditioned Medium. (E–F) Tau Expression in L-Glu Injured-N2A with BV2 and RAW264.7 Conditioned Medium. L-Glu: L-Glutamic acid. The d.d.H$_2$O was considered as a control.
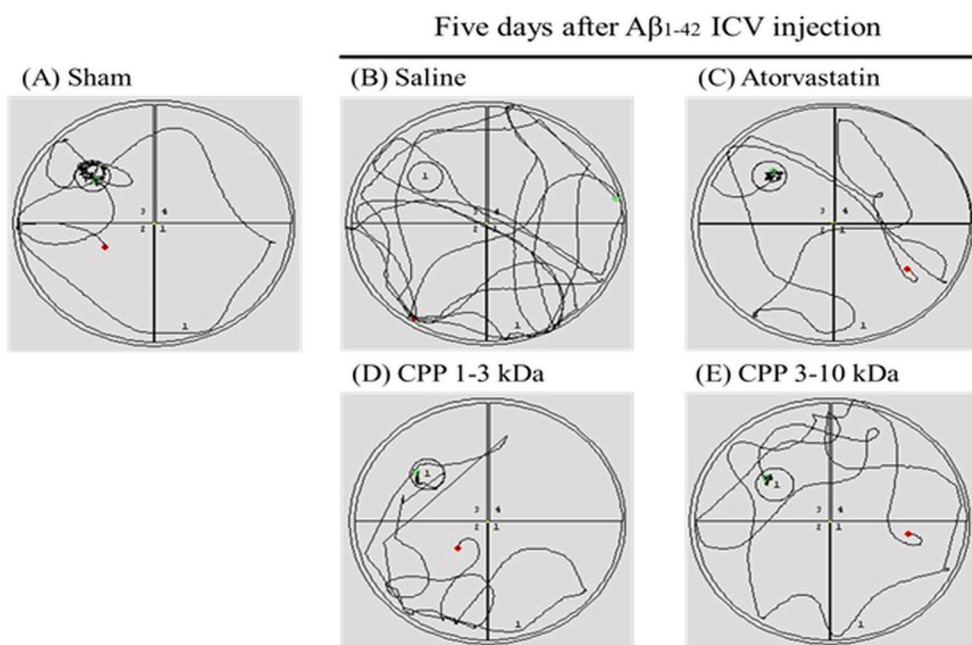

Fig. 7. Water maze behavior assay and evaluation of spatial learning and memory by (A) Sham, (B) Saline, (C) Atorvastatin), (D) 1–3 kDa (100 mg/kg), (E) CPP 3–10 kDa (100 mg/kg) treated mice (n = 6) through searching for the target quadrant and swimming path through other quadrants (each test time limit is 180 s). Mice were fed with different subjects for 14 days and then injected with Aβ$_{1-42}$ (5 μM) into the brain to induce neurotoxicity, and after 5 days, the mouse water maze behavior assay was performed.

bioactive peptides and therefore represents a strong pharmaceutical profile [45]. Notably, *Chlorella pyrenoidosa* hydrolyzed protein has shown antioxidant properties with anti-atherosclerosis potential [46]. It has also been found effective in downregulating LPS-induced inflammation and NO production [47]. Considering the therapeutic significance of *Chlorella pyrenoidosa,* we extracted *Chlorella pyrenoidosa* peptides (CPPs) of different molecular weight (<1 kDa, 1–3 kDa, 3–10 kDa, and >10 kDa) and evaluated various parameters
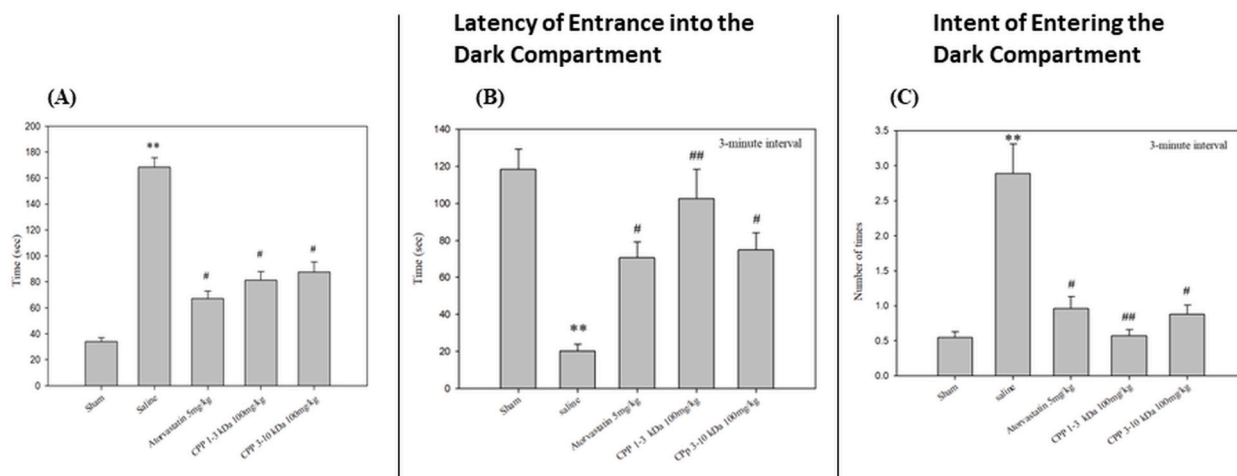
Fig. 8. Mouse water maze behavior assay. (A) Search for hidden platform (B) Latency of entrance into the dark compartment and (C) Intention of entering dark compartment by Sham, Saline, Atorvastatin, CPP 1–3 kDa (100 mg/kg), and CPP 3–10 kDa (100 mg/kg)-treated groups. Number of animals (n) = 6. **$P < 0.01$ compared with sham, #$P < 0.05$ compared with saline.
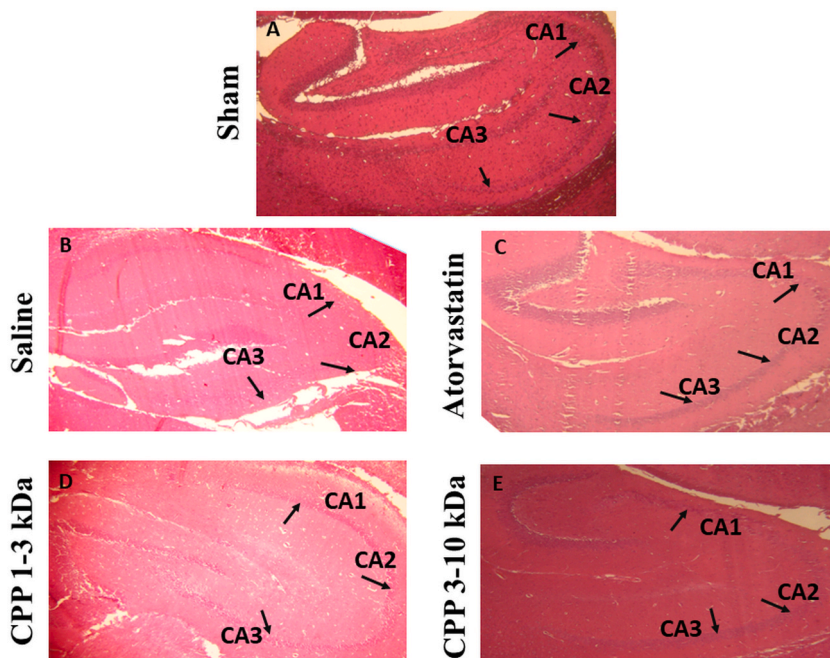

Fig. 9. Representative photomicrographs of mouse hippocampal CA1-CA3 regions of (A) Sham, (B) Saline, (C) Atorvastatin, (D) 1–3 kDa (100 mg/kg), (E) CPP 3–10 kDa (100 mg/kg) (n = 6).

in vitro as well as *in vivo*.

Our MTT results indicated that CPPs at 1000 μg/ml concentration is more toxic than 100 μg/ml. While based on size, CPP >10 kDa has been found most toxic at both concentrations among all CPPs. Thus, considering the lower cytotoxicity, we selected 100 μg/ml as the optimum concentration for further study. Notably, the hydrolyzed peptide of molecular weight 3–5 kDa at a concentration of 160 μg/ml from *Chlorella vulgaris* has been found to effectively inhibit the growth of cancerous MCF-1 cell lines [48]. Further, CPPs of 3–5 and 5–10 kDa size have been shown to exert inhibitory activity against the human liver HepG2 cancer cell line [49]. Moreover, microencapsulation and encapsulation further improved the inhibitory effect of polypeptides. Similarly, methanolic extract of both *Chlorella vulgaris AS-13* and *Chlorella pyrenoidosa AS-6* have demonstrated an inhibitory effect on WRL68 (normal cell hepatic cell line), MCF7 (breast cancer cell), and cancer cell lines HepG2 at 92 μg/ml and 87 μg/ml, respectively [50]. In addition, methanolic extracts *Chlorella pyrenoidosa* AS-6 also showed a positive impact on WRL-68 cell lines. Thus, these studies imply the inhibitory concentration of

CPPs for their therapeutic potential.

We further assessed the effect of CPPs on $A\beta_{1-42}$-induced cytotoxicity in N2A cells. From the amyloid precursor protein (APP), $A\beta_{39-43}$ residue polypeptide, is cleaved via β- and γ-secretases. The predominant Aβ species end at 40 and 42 residues possess a greater aggregation affinity and are contemplated more neurotoxic due to two additional hydrophobic amino acids [51]. In our study, N2A cellular toxicity was induced by $A\beta_{1-42}$ (10 μM), which was improved through the addition of CPP, with the strongest effect by 3–10 kDa showing the highest improvement. Similar to our results, the extracts of *Chlorella vulgaris* at concentrations between 200 and 1000 μg/ml significantly maintained the cell viability of human neuroblastoma SH-SY5Y cells [52]. In addition, hot water extract of *Chlorella vulgaris* may induce the proliferation of intestinal epithelial cells (IEC-6) via activation of MAPK, PI3K/Akt, and canonical Wnt signaling pathways. Thus, our studies indicate that CPPs possess the potential to maintain the cell viability of neuronal cells even in $A\beta_{1-42}$ induced stress. Further, LPS, BV2, and RAW264.7 conditioned medium releases proinflammatory and neurotoxic factors such as IL-1β, IL-6, iNOS, PGE2, COX-2, NF-κB and TNF-α [53]. In this line, the exposure of N2A cells to LPS, BV2, and RAW264.7 conditioned medium increased the inflammatory and oxidative stress on neuronal cells. In our study, CPPs have been found significantly effective in maintaining the cell viability of N2A cells pre-exposed to $A\beta_{1-42}$ (10 μM) toxicity, and the cell medium is replaced with BV2 and BV2+RAW264.7 conditioned medium. Similar to our microalgal-based study, a report evidenced that the ethanol extract (20 μg/mL) and hexane layer of ethanol extract (20 μg/mL) of microalgae *Aurantiochytrium* sp. has been found effective in inhibiting Aβ-induced cell death of SH-SY5Y neural cell lines [54]. In addition, intracellular ATP level was also increased following the treatment. The Aβ induces oxidative stress and causes mitochondrial dysfunction resulting in decreased intracellular ATP levels. In a seminal study, using MTT assay of carotenoids-enriched extracts from microalgae *Haematococcus pluvialis*, *Porphyridium cruentum*, *Nannochloropsis oceanica* and *Tisochrysis lutea* on Tubular epithelial cells (HK-2), human THP-1 monocytes and human SH-SY5Y neuroblastoma cell lines reported that only *H. pluvialis* and *T. lutea* extract at 100 μg/mL are toxic to HK-2 cell line while all the microalgae extracts were found not cytotoxic for any cell lines at concentrations ranging from 25 to 50 μg/mL [55]. These results indicate a safer profile of CPP as well as other microalgae extracts for the neuronal cell line.

We further evaluated to determine the anti-inflammatory profile of CPPs. Initially, the inflammatory stress was induced by exposing cell lines to LPS (2 μg/ml), $A\beta_{1-42}$ (10 μM), and L-Glutamic acid (2 mM). The LPS-mediated inflammatory response was measured by determining the level of PGE2, IL-6, and iNOS levels in BV2 and N2A cell lines. No significant effect of glutamic acid (2 mM), and $A\beta_{1-42}$ (10 μM) on the level of inflammatory factors PGE2, IL-6, and iNOS in N2A cells. However, CPPs exerted a considerable impact on the level of these inflammatory factors in BV2 cells. CPP 1–3 kDa, 3–10 kDa, and 3–10 kDa significantly lowered PGE2, IL-6, and iNOS levels in LPS-induced BV2 cell lines. The accumulative effectiveness of CPP in lowering LPS-induced stress in BV2 cells in comparison to atorvastatin (10 μM) is significantly higher (Fig. 3). Similarly, the increased level of TNF-α, COX-2, and IL-1β in LPS (2 μg/ml) induced RAW264.7 cell lines was significantly reduced. All groups of CPPs significantly suppressed TNF-α levels and the effectiveness of CPPs is significantly higher than atorvastatin (10 μM). CPP 3–10 kDa and >10 kDa showed a significantly lower COX-2 expression compared to other bioactive CPPs. Additionally, CPP 1–3 kDa significantly lowers the expression of IL-1β in LPS-induced RAW264.7 cell lines. In line with our results, carotenoid-enriched microalgae extract of *H. pluvialis*, *P. cruentum, T. lutea,* and *N. oceanica* also reduced the antioxidant and anti-inflammatory stress in human neuroblastoma cell line SH-SY5Y [55]. The previous report has revealed that ethanol extract of *Nannochloropsis oceanica (N. oceanica)* at 20 μg/mL concentration downregulated the nitric oxide synthesis, NF-κB and β-secretase activity in LPS-induced BV2, RAW264.7, and neuronal cells [56].

Carotenoid-Rich Extract from Chlorella (*Parachlorella beijerinckii*) significantly downregulated the expression of IL-1, IFNB1, NoS2, IL-1β, and IL-6 in mouse macrophage RAW264.7 cell line [57]. This extract significantly inhibited mitochondrial ROS production after NLRP3 inflammation. A remarkable suppression of NO production, iNOS, NF-κB, TNF-α, and PGE2 by Chlorella-11 peptide (Val--Glu-Cys-Tyr-Gly-Pro-Asn-Arg-Pro-Gln-Phe) in LPS-induced RAW264.7 cells [47]. Moreover, *N. oceanica* mediated *in vivo* down-regulation of APP and BACE1 expression triggers suppression of $A\beta_{1-42}$ synthesis [56]. Our results also confirm that CPP 3–10 kDa at 100 μg/mL has been found most effective in downregulating the inflammatory markers IL-6 and TGF-β in BV2 and TNF-α and NF-κβ in RAW264.7 cell lines. Thus, the potential of bioactive peptides and extract from *chlorella* sp. could be an effective way to alleviate the oxidative, and inflammatory stress in Alzheimer's and other neurodegenerative disorders.

Further, similar to our *in vivo* results, a previous study revealed that a microalgae *Dunaliella salina* containing zeaxanthin is efficacious in reducing the level of IL-1β, iNOS, neurotransmitters (norepinephrine, serotonin, and dopamine), Aβ protein and myelin basic protein in rat brain [58]. Another bioactive compound fucoxanthin extracted from microalgae *Phaeodactylum tricornutum* inhibits the aggregation and accumulation of oligomeric Aβ and hyperphosphorylated tau in APP/PS1 transgenic mice [59]. Fucoxanthin has also been found effective in inhibiting NLRP3 inflammasome activation, pro-inflammatory cytokine IL-6, IL-1β, and TNF-α [59]. It also suppresses the priming step of inflammation via downregulating the level of pro-IL-1β and phosphorylated IκB-α expression. In LPS-injected mice, the enhanced Aβ accumulation in the brain has been significantly lowered by the administration of *N. oceanica* extract [56]. In addition, the ethanolic extract of *N. oceanica* also reduced amyloidogenesis and neuroinflammation via downregulating the NF-κB signaling pathway. Similarly, yessotoxin (1 nM) extracted from another microalga *Protoceratium reticulatum* demonstrated its anti-Alzheimer activity *in vitro* by lowering the accumulation of Tau and its hyperphosphorylation [60].

The efficacy of CPPs in restoring spatial memory and learning is determined by the MWM behavior test. Our results demonstrated that CPP 1–3 kDa and 3–10 kDa are effective in improving spatial memory and learning which is comparable to atorvastatin. Further, CPPs also reduce the latency in searching hidden platforms and the intention of the entrance to the dark compartment with electric shock which is comparable to atorvastatin. In an important study, the microalgae *Aurantiochytrium* sp. extracts significantly lowered escape latency in SAMP8 mice on 6 and 7 days of training [54]. *Chlorella vulgaris* has been effective in reversing nicotine-induced brain damage, oxidative stress, DNA damage, inflammation stress, and microstructural changes in the brain tissue of mice models [61]. Moreover, *C. vulgaris* may significantly improve the neurobehavioral response of Ehrlich ascites carcinoma (EAC) Swiss female mice

which was evidenced through behavioral tests such as swimmer performance, open field, posture tail suspension, and reflex inclined plain tests. The therapeutic impact of *C. vulgaris* is associated with its potential to prevent brain damage by regulating the level of neurotransmission by its bioactive molecules such as carotenes, flavonoids, peptides, and polysaccharides. Another microalgae *Chlorella sorokiniana* has also been found effective in improving short-term memory due to the elevation of noradrenaline (NA) and serotonin (5-HT) content in the hippocampus only [62]. However, no significant difference in exploratory performance, depressive-like behavior, locomotor activity, and anxiety profile was observed. Further, *Spirulina* sp. consumption significantly improves cognitive skills, mental fatigue, and language in malnourished children [62,63]. Moreover, *Spirulina* sp. microalgae prevent cerebrovascular pathology by regulating internal pressure and providing safety to the vascular wall of brain vessels from endothelial damage [63]. It has also been observed that ethanol extracts of *Chlorella sorokiniana* and *Chlorella minutissima* are effective in preventing the $A\beta_{1-42}$ aggregation [31]. Similarly, *Spirulina maxima* extract lowers the hippocampal $A\beta_{1-42}$ and suppresses the processing of factors associated with the amyloid precursor protein, and improves cognitive ability in $A\beta_{1-42}$ injected mice via inhibiting the increased phosphorylation of glycogen synthase kinase-3β [64].

In our study, CPP 1–3 kDa and CPP 3–10 kDa were effective in restoring cell loss in the CA1 and CA3 regions of the mouse hippocampus. In line with our study, a similar effect of *Dunaliella salina* extracts and its component zeaxanthin was observed in terms of inhibition of degenerated hippocampal neurons in CA1 hippocampal regions [58]. Whereas the ethanol extract of *N. oceanica* has been found effective in lowering the number of GFAP reactive cells in the cortex and hippocampus of LPS-injected mice brains, leading to improved cognitive ability [56]. Moreover, similar to previous microalgal-based study, the cytoprotective effects of CPP 1–3 kDa and CPP 3–10 kDa may be achieved through their penetration of blood-brain barrier [23]. This result is supported by a clinical study showing the effectiveness of Chlorella Sp. i.e. *Chlorella vulgaris* extract (CVE) in significantly reduced Hospital Anxiety and Depression Scale (HADS) and Beck Depression Inventory II (BDI-II) scale in a major depressive disorder without any significant adverse events [65]. This therapeutic effect of CVE could be associated with its potential to proliferate stem cells, lowering oxidative stress, the presence of sporopollenin (neurotoxin-binding molecules), and neuroprotective molecule such as methyl cobalamine, alpha-and gamma-linoleic acids [65,66]. Another clinical study demonstrated that Chlorella supplementation enhanced plasma lutein levels and significantly reduced phospholipid hydroperoxide (PLOOH), a contributing factor for Alzheimer's disease, in erythrocyte membranes [67]. The finding of the study indicates the potential of *Chlorella* in reducing oxidative stress and potential benefits in AD treatment. Interestingly, the *Chlorella pyrenoidosa* water extract showed anti-aging effects of *Chlorella pyrenoidosa* especially in the healthy individuals. The impacts were mediated by significantly downregulated inducible nitric oxide synthase (iNOS) and cyclooxygenase-2 (COX-2), and improved antioxidant levels (SOD, CAT TEAC, and DHEAs) and suppressed oxidative stress/aging markers (TBARS and 8-OHdG) in addition to protecting liver (reduced oxaloacetic transaminase and serum glutamic pyruvic transaminase) [68]. As per a clinical report, the daily consumption of chlorella can remarkably inhibit total cholesterol, very low-density lipoprotein cholesterol, apolipoprotein B, triglycerides, in mild hypercholesterolemic adults [69]. These studies demonstrate the potential clinical implications of CPP in AD.

5. Conclusions

Our study demonstrates that CPPs specifically CPP 1–3 kDa and CPP 3–10 kDa could be further explored as effective candidates for AD therapy. CPPs at 100 μg/mL have shown a significant improvement in cell density in the CA1-CA3 hippocampal region, spatial memory, and a significant reduction in inflammatory stress in experimental mice. Taken together, the *in vivo* and *in vitro* findings of our study indicate the strong potential of CPPs in alleviating AD pathology through anti-inflammatory, and anti-amyloid activities via reducing APP and tau NFT. However, more pre-clinical and clinical studies are required to evaluate the significance of CPPs in developing effective and safe treatment of AD and related neurodegenerative disorders.

Author contribution statement

Shu-Mei Wang: Conceived and designed the experiments; Performed the experiments; Analyzed and interpreted the data; Wrote the paper.

Jiunn-Jye Chuu, Ching-Kuo Lee, Chia-Yu Chang: Analyzed and interpreted the data; Contributed reagents, materials, analysis tools or data.

Funding statement

Data availability statement

Data will be made available on request.

Declaration of interest's statement

The authors declare no conflict of interest.

Appendix A. Supplementary data

Supplementary data to this article can be found online at https://doi.org/10.1016/j.heliyon.2023.e15406.

References

[1] Z. Breijyeh, R. Karaman, Comprehensive review on Alzheimer's disease: causes and treatment, Molecules (24) (2020) 25.
[2] X. Sun, W.-D. Chen, Y.-D. Wang, β-Amyloid: the key peptide in the pathogenesis of Alzheimer's disease, Front. Pharmacol. (2015) 6.
[3] T. Guo, et al., Molecular and cellular mechanisms underlying the pathogenesis of Alzheimer's disease, Mol. Neurodegener. 15 (1) (2020) 40.
[4] A.s. Association, 2016 Alzheimer's disease facts and figures, Alzheimer's Dementia 12 (4) (2016) 459–509.
[5] W.S. Weidner, P. Barbarino, P4-443: the state of the art of dementia research: new frontiers, Alzheimer's Dementia (2019) 15.
[6] 2021 Alzheimer's disease facts and figures, Alzheimers Dement 17 (3) (2021) 327–406.
[7] R. Medeiros, D. Baglietto-Vargas, F.M. LaFerla, The role of tau in Alzheimer's disease and related disorders, CNS Neurosci. Ther. 17 (5) (2011) 514–524.
[8] S. Sadigh-Eteghad, et al., Amyloid-beta: a crucial factor in Alzheimer's disease, Med. Princ. Pract. 24 (1) (2015) 1–10.
[9] G.-f. Chen, et al., Amyloid beta: structure, biology and structure-based therapeutic development, Acta Pharmacol. Sin. 38 (9) (2017) 1205–1235.
[10] F. Olsson, et al., Characterization of intermediate steps in amyloid beta (Aβ) production under near-native conditions, J. Biol. Chem. 289 (3) (2014) 1540–1550.
[11] M. Takami, et al., γ-Secretase: successive tripeptide and tetrapeptide release from the transmembrane domain of β-carboxyl terminal fragment, J. Neurosci. 29 (41) (2009) 13042–13052.
[12] G.S. Bloom, Amyloid-β and tau: the trigger and bullet in Alzheimer disease pathogenesis, JAMA Neurol. 71 (4) (2014) 505–508.
[13] A. Viswanathan, S.M. Greenberg, Cerebral amyloid angiopathy in the elderly, Ann. Neurol. 70 (6) (2011) 871–880.
[14] M.Y. Aksenov, et al., Enhancement of β-amyloid peptide Aβ (1–40)-mediated neurotoxicity by glutamine synthetase, J. Neurochem. 65 (4) (1995) 1899–1902.
[15] S.M. Yatin, M. Aksenov, D.A. Butterfield, The antioxidant vitamin E modulates amyloid β-peptide-induced creatine kinase activity inhibition and increased protein oxidation: implications for the free radical hypothesis of Alzheimer's disease, Neurochem. Res. 24 (3) (1999) 427–435.
[16] R.J. Mark, et al., Amyloid beta-peptide impairs ion-motive ATPase activities: evidence for a role in loss of neuronal Ca2+ homeostasis and cell death, J. Neurosci. 15 (9) (1995) 6239–6249.
[17] M. Ezeani, M. Omabe, A new perspective of lysosomal cation channel-dependent homeostasis in Alzheimer's disease, Mol. Neurobiol. 53 (3) (2016) 1672–1678.
[18] S. Varadarajan, et al., Alzheimer's amyloid β-peptide-associated free radical oxidative stress and neurotoxicity, J. Struct. Biol. 130 (2–3) (2000) 184–208.
[19] S. Weggen, et al., A subset of NSAIDs lower amyloidogenic Aβ42 independently of cyclooxygenase activity, Nature 414 (6860) (2001) 212–216.
[20] S. Liu, et al., TLR2 is a primary receptor for Alzheimer's amyloid β peptide to trigger neuroinflammatory activation, J. Immunol. 188 (3) (2012) 1098–1107.
[21] M.T. Heneka, D.T. Golenbock, E. Latz, Innate immunity in Alzheimer's disease, Nat. Immunol. 16 (3) (2015) 229–236.
[22] U. Neniskyte, J.J. Neher, G.C. Brown, Neuronal death induced by nanomolar amyloid β is mediated by primary phagocytosis of neurons by microglia, J. Biol. Chem. 286 (46) (2011) 39904–39913.
[23] T.A. Olasehinde, A.O. Olaniran, A.I. Okoh, Therapeutic potentials of microalgae in the treatment of Alzheimer's disease, Molecules (3) (2017) 22.
[24] T.B. Ali, et al., Adverse effects of cholinesterase inhibitors in dementia, according to the pharmacovigilance databases of the united-states and Canada, PLoS One (12) (2015) 10.
[25] M.F. de Jesus Raposo, R.M. de Morais, A.M. de Morais, Health applications of bioactive compounds from marine microalgae, Life Sci. 93 (15) (2013) 479–486.
[26] S. Guzmán, A. Gato, J.M. Calleja, Antiinflammatory, analgesic and free radical scavenging activities of the marine microalgae Chlorella stigmatophora and Phaeodactylum tricornutum, Phytother Res. 15 (3) (2001) 224–230.
[27] E. Gardeva, et al., Cancer protective action of polysaccharide, derived from red microalga Porphyridium cruentum—a biological background, Biotechnol. Biotechnol. Equip. 23 (sup1) (2009) 783–787.
[28] K.N. Chidambara Murthy, et al., In vivo antioxidant activity of carotenoids from Dunaliella salina–a green microalga, Life Sci. 76 (12) (2005) 1381–1390.
[29] M. Huheihel, et al., Activity of Porphyridium sp. polysaccharide against herpes simplex viruses in vitro and in vivo, J. Biochem. Biophys. Methods 50 (2) (2002) 189–200.
[30] Y. Nakashima, et al., Preventive effects of Chlorella on cognitive decline in age-dependent dementia model mice, Neurosci. Lett. 464 (3) (2009) 193–198.
[31] T.A. Olasehinde, et al., Chlorella sorokiniana and Chlorella minutissima exhibit antioxidant potentials, inhibit cholinesterases and modulate disaggregation of β-amyloid fibrils, Electron. J. Biotechnol. 40 (2019) 1–9.
[32] Y. Li, et al., Investigation of chlorella pyrenoidosa protein as a source of novel angiotensin I-converting enzyme (ACE) and dipeptidyl peptidase-IV (DPP-IV) inhibitory peptides, Nutrients (5) (2021) 13.
[33] X. Fan, et al., Marine algae-derived bioactive peptides for human nutrition and health, J. Agric. Food Chem. 62 (38) (2014) 9211–9222.
[34] R.E. Merchant, C.A. Andre, A review of recent clinical trials of the nutritional supplement Chlorella pyrenoidosa in the treatment of fibromyalgia, hypertension, and ulcerative colitis, Alternative Ther. Health Med. 7 (3) (2001) 79–92.
[35] J.-Y. Cherng, M.-F. Shih, Preventing dyslipidemia by Chlorella pyrenoidosa in rats and hamsters after chronic high fat diet treatment, Life Sci. 76 (26) (2005) 3001–3013.
[36] T. Senthilkumar, N. Sangeetha, N. Ashokkumar, Antihyperglycemic, antihyperlipidemic, and renoprotective effects of Chlorella pyrenoidosa in diabetic rats exposed to cadmium, Toxicol. Mech. Methods 22 (8) (2012) 617–624.
[37] H.S. Nhan, K. Chiang, E.H. Koo, The multifaceted nature of amyloid precursor protein and its proteolytic fragments: friends and foes, Acta Neuropathol. 129 (1) (2015) 1–19.
[38] M.P. Murphy, H. LeVine 3rd, Alzheimer's disease and the amyloid-beta peptide, J Alzheimers Dis 19 (1) (2010) 311–323.
[39] T. Bayer, O. Wirths, Intracellular accumulation of amyloid-beta - a predictor for synaptic dysfunction and neuron loss in Alzheimer's disease, Front. Aging Neurosci. (2010) 2.
[40] F.C. Lau, Attenuation of iNOS and COX2 by blueberry polyphenols is mediated through the suppression of NF-kB activation, J. Funct.Foods 1 (3) (2009) 274–283.
[41] Y. Wang, et al., Forsythiaside A exhibits anti-inflammatory effects in LPS-stimulated BV2 microglia cells through activation of Nrf2/HO-1 signaling pathway, Neurochem. Res. 41 (4) (2016) 659–665.
[42] C. Wang, et al., Neuroprotective effects of verbascoside against Alzheimer's disease via the relief of endoplasmic reticulum stress in Aβ-exposed U251 cells and APP/PS1 mice, J. Neuroinflammation 17 (1) (2020) 309.
[43] P. Scheltens, et al., Alzheimer's disease, Lancet 397 (10284) (2021) 1577–1590.
[44] R.P. Parameswari, T. Lakshmi, Microalgae as a potential therapeutic drug candidate for neurodegenerative diseases, J. Biotechnol. 358 (2022) 128–139.
[45] L.A. Tejano, et al., Prediction of bioactive peptides from chlorella sorokiniana proteins using proteomic techniques in combination with bioinformatics analyses, Int. J. Mol. Sci. 20 (7) (2019) 1786.
[46] Y. Liu, et al., Antioxidative effect of chlorella pyrenoidosa protein hydrolysates and their application in krill oil-in-water emulsions, Mar. Drugs (6) (2022) 20.
[47] J.Y. Cherng, et al., Beneficial effects of Chlorella-11 peptide on blocking LPS-induced macrophage activation and alleviating thermal injury-induced inflammation in rats, Int. J. Immunopathol. Pharmacol. 23 (3) (2010) 811–820.
[48] M. Sedighi, et al., Potential health effects of enzymatic protein hydrolysates from chlorella vulgaris, Applied Food Biotechnology 3 (3) (2016) 160–169.
[49] X. Wang, X. Zhang, Separation, antitumor activities, and encapsulation of polypeptide from Chlorella pyrenoidosa, Biotechnol. Prog. 29 (3) (2013) 681–687.

[50] V. Kalebar, S. Raikar, S. Adhoni, SCREENING OF PHARMACOLOGICAL AND CYTOTOXIC ACTIVITIES OF FRESH WATER LAKE ISOLATED MICROALGAE CHLORELLA VULGARIS AS-13 AND CHLORELLA PYRENOIDOSA AS-6. (2018).

[51] E. Tamagno, et al., The unexpected role of aβ1-42 monomers in the pathogenesis of Alzheimer's disease, J Alzheimers Dis 62 (3) (2018) 1241–1245.

[52] S. Norfaizatul, et al., Dual effects of plant antioxidants on neuron cell viability. (2010).

[53] P. Dowling, M. Clynes, Conditioned media from cell lines: a complementary model to clinical specimens for the discovery of disease-specific biomarkers, Proteomics 11 (4) (2011) 794–804.

[54] K. Sasaki, et al., Microalgae Aurantiochytrium sp. Increases neurogenesis and improves spatial learning and memory in senescence-accelerated mouse-prone 8 mice, Front. Cell Dev. Biol. (2021) 8.

[55] R. Gallego, et al., Anti-inflammatory and neuroprotective evaluation of diverse microalgae extracts enriched in carotenoids, Algal Res. 67 (2022) 102830.

[56] J.Y. Choi, et al., Inhibitory effect of ethanol extract of Nannochloropsis oceanica on lipopolysaccharide-induced neuroinflammation, oxidative stress, amyloidogenesis and memory impairment, Oncotarget 8 (28) (2017) 45517–45530.

[57] Y. Nakashima, et al., Attenuating effect of chlorella extract on NLRP3 inflammasome activation by mitochondrial reactive oxygen species, Front. Nutr. (2021) 8.

[58] F.K. El-Baz, et al., Dunalialla salina microalgae and its isolated zeaxanthin mitigate age-related dementia in rats: modulation of neurotransmission and amyloid-β protein, Toxicol Rep 8 (2021) 1899–1908.

[59] A.H. Lee, et al., Fucoxanthin from microalgae Phaeodactylum tricornutum inhibits pro-inflammatory cytokines by regulating both NF-κB and NLRP3 inflammasome activation, Sci. Rep. 11 (1) (2021) 543.

[60] A. Saide, et al., Unlocking the health potential of microalgae as sustainable sources of bioactive compounds, Int. J. Mol. Sci. (9) (2021) 22.

[61] A.A.-R. Mohamed, et al., Sustained functioning impairments and oxidative stress with neurobehavioral dysfunction associated with oral nicotine exposure in the brain of a murine model of Ehrlich ascites carcinoma: modifying the antioxidant role of chlorella vulgaris, Biology 11 (2) (2022) 279.

[62] M.G. Morgese, et al., Chlorella sorokiniana extract improves short-term memory in rats, Molecules (10) (2016) 21.

[63] V. Sorrenti, et al., Spirulina microalgae and brain health: a scoping review of experimental and clinical evidence, Mar. Drugs (6) (2021) 19.

[64] E.-J. Koh, et al., Spirulina maxima extract ameliorates learning and memory impairments via inhibiting GSK-3β phosphorylation induced by intracerebroventricular injection of amyloid-β 1–42 in mice, Int. J. Mol. Sci. 18 (11) (2017) 2401.

[65] Y. Panahi, et al., A randomized controlled trial of 6-week Chlorella vulgaris supplementation in patients with major depressive disorder, Compl. Ther. Med. 23 (4) (2015) 598–602.

[66] H. Eyre, B.T. Baune, Neuroplastic changes in depression: a role for the immune system, Psychoneuroendocrinology 37 (9) (2012) 1397–1416.

[67] T. Miyazawa, et al., Ingestion of Chlorella reduced the oxidation of erythrocyte membrane lipids in senior Japanese subjects, J. Oleo Sci. 62 (11) (2013) 873–881.

[68] H.F. Chiu, et al., Beneficial effect of Chlorella pyrenoidosa drink on healthy subjects: a randomized, placebo-controlled, double-blind, cross-over clinical trial, J. Food Biochem. (4) (2021) 45.

[69] N.H. Ryu, et al., Impact of daily Chlorella consumption on serum lipid and carotenoid profiles in mildly hypercholesterolemic adults: a double-blinded, randomized, placebo-controlled study, Nutr. J. 13 (1) (2014) 57.